



13 April 2001

**CHEMICAL
PHYSICS
LETTERS**

Chemical Physics Letters 338 (2001) 14–20

www.elsevier.nl/locate/cplett

In-plane-aligned membranes of carbon nanotubes

D.A. Walters, M.J. Casavant, X.C. Qin, C.B. Huffman, P.J. Boul, L.M. Ericson,
E.H. Haroz, M.J. O'Connell, K. Smith, D.T. Colbert *, R.E. Smalley

*Departments of Chemistry and Physics, The Center for Nanoscale Science and Technology, Rice University,
MS-100, P.O. Box 1892, Houston, TX 77251-1892, USA*

Received 15 October 2000

Abstract

We have produced the first macroscopic objects comprised of highly aligned single-wall carbon nanotubes (SWNTs). These objects are thin membranes prepared by producing a suspension of SWNT segments, introducing the suspension to a strong magnetic field to align the segments, and filtering the suspension in the magnetic field to produce an aligned membrane of SWNT. These membranes exhibited natural cleavage planes parallel to the magnetic field. This preparation of macroscopic samples of aligned single-wall nanotubes permits exploitation of their highly anisotropic properties, and will enable measurement of the electronic, thermal, magnetic, mechanical, and optical properties of bulk nanotube materials. © 2001 Elsevier Science B.V. All rights reserved.

1. Introduction

Single-wall carbon nanotubes (SWNTs) are prized for their mechanical, electrical, thermal, and chemical properties. Early theoretical predictions of these properties have been substantially verified experimentally as high quality material has become available. Macroscopic materials comprising large number of nanotubes in crystalline alignment with one another would constitute highly anisotropic material with a wide range of potential applications. We report here the first realization of a macroscopic sample comprising substantially aligned SWNT.

The aligned nanotube sample produced in the present experiment was created by aligning suspended SWNT segments in a strong magnetic field

and filtering them out of suspension while they remain aligned by the magnetic field. SWNTs have been predicted to have an anisotropic magnetic susceptibility [1]. The lowest energy orientation for all SWNT types is parallel to the field, \mathbf{B} . Application of a sufficiently strong magnetic field should therefore orient nanotubes that are free to rotate in a liquid suspension [1]; a process similar to the magnetic orientation of liquid crystals [2]. Magnetic alignment has already been demonstrated for small quantities of multi-wall nanotubes [3]. Calculations reveal that metallic SWNTs (such as the (n, n) variety) are paramagnetic in the direction of their long axes, and tend to align parallel to the ambient magnetic field. The other varieties of SWNT are diamagnetic, but their diamagnetic susceptibilities are most negative in the direction perpendicular to the tube axis, causing them to also align parallel to the direction of an ambient field. The alignment energies for both the paramagnetic and diamagnetic varieties of SWNT are

* Corresponding author. Fax: +1-713-285-5320.

E-mail address: colbert@rice.edu (D.T. Colbert).

comparable, and calculated SWNT susceptibilities [1,4–8] predict that at room temperature, fields of the order of 10 T will produce an observable alignment in a liquid suspension of individual SWNT.

For example, the predicted molar susceptibilities for a (10,10) nanotube are: $\chi_{\parallel}^m = +85.4 \times 10^{-6}$ emu (mol C) $^{-1}$ when parallel to \mathbf{B} , and $\chi_{\perp}^m = -21.0 \times 10^{-6}$ emu (mol C) $^{-1}$ when perpendicular. The alignment energy is small enough, however, that we must consider the effects of thermal energy. The potential energy U of a nanotube containing n moles of carbon is $U(\theta) = -B^2 n (\chi_{\parallel}^m \cos^2 \theta + \chi_{\perp}^m \sin^2 \theta)$, where θ is the angle between the nanotube axis and the magnetic field. Each nanotube undergoes Brownian motion in this potential with an average energy of $k_B T$, where $T = 287 \pm 3$ K for the experiments reported here. Maxwell–Boltzmann statistics gives the dis-

tribution of nanotube orientations: $dP(\theta) = (v)^{-1} u \times \exp(-u^2 \sin^2 \theta) \sin \theta d\theta$, in which $u = \sqrt{\Delta U / (k_B T)}$ and $v = F(u)$, where F is Dawson's integral [9], and the alignment energy is $\Delta U = U(\pi/2) - U(0) = B^2 n (\chi_{\parallel}^m - \chi_{\perp}^m)$. ΔU must be many times $k_B T$ in order to obtain good alignment of nanotubes. For a (10,10) nanotube of length 300 nm, a field of 15.3 T, achievable in the laboratory, gives $\Delta U = 5 k_B T$ using the susceptibilities above.

2. Experimental

To test whether fields of the order of 10 T give substantial alignment of suspended SWNT, we passed polarized light through a (10 mg/l) nanotube suspension in dimethylformamide in a magnetic field (Fig. 1). These SWNTs were produced by the

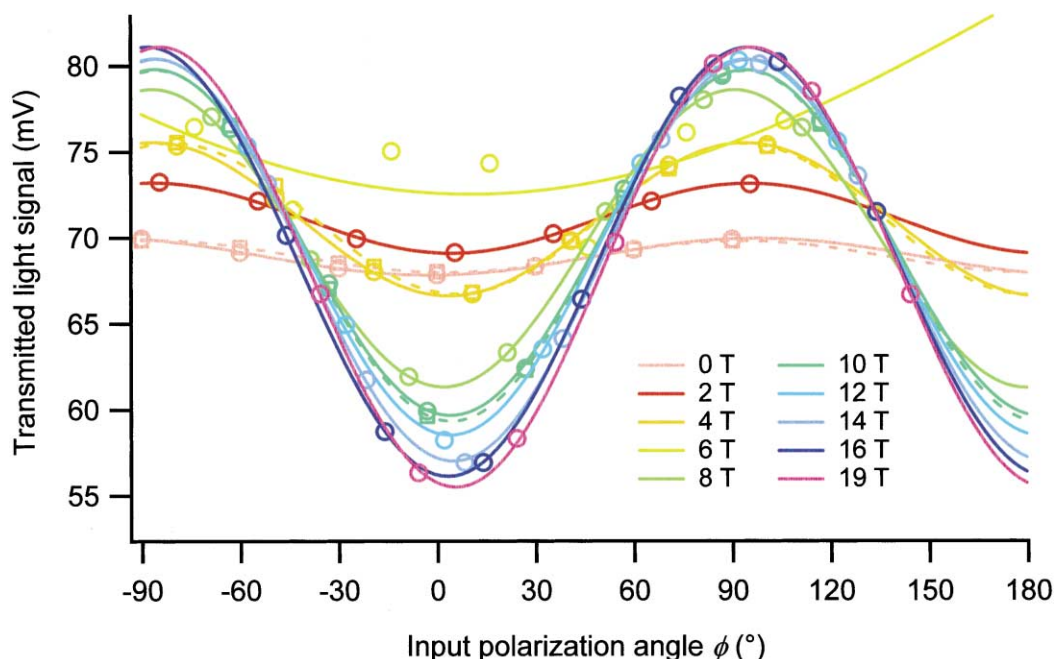


Fig. 1. Polarized light was passed through a suspension of SWNTs in dimethylformamide and the transmitted light collected. A magnetic field was applied perpendicular to the propagation direction of the light. The transmittance was monitored as a function of the incident polarization angle ϕ , the angle between the incident light electric field vector and the magnetic field. Solid lines are sinusoidal fits to the measured transmitted light intensities. As the field was increased from zero, a significant (up to 37% peak-to-peak) modulation of the light intensity developed. Minimum transmittance occurred when the incident light was polarized parallel to the magnetic field. Therefore the SWNTs were aligned along \mathbf{B} . No permanent change to the suspension occurred. The squares and dashed lines correspond to the data (and fits to it) measured while decreasing values of the field to zero, and agree well with the other data, which were taken at successively higher values of the field as the magnet current was increased.

laser-oven method [10], purified [11] and suspended in dimethylformamide by extensive sonication. About 3 ml of suspension was placed in a cuvette held in the bore of a 19 T, 195 mm bore DC resistive electromagnet at the National High Magnetic Field Laboratory in Tallahassee, FL. A homebuilt optical system delivered a polarized HeNe laser beam to the cuvette and steered the transmitted light to a Si photodiode. A half-wave plate was used to rotate the polarization of the incident light. A control experiment with pure dimethylformamide in the cuvette showed negligible ($<0.7\%$) variations in intensity as the half-wave plate was rotated, regardless of the magnetic field.

As the polarization of the incident light was rotated, the sample's transmittance varied sinusoidally, and the amplitude of this modulation increased with the applied magnetic field (Fig. 1). The small residual modulation at zero field is most likely due to slightly polarizing reflections from the beamsteering optics. The transmittance was a minimum when the electric vector, ϵ , of the incident light was parallel to \mathbf{B} [12].

The peak-to-peak modulation M saturates at high magnetic fields (Fig. 2). Using the model described below for the absorption and scattering of light from an ensemble of nanotubes with a distribution of orientations, we infer that at 19 T nanotubes have on average an alignment energy 28 ± 3 times $k_B T$. This corresponds to 90% of the tubes having axial orientations within $17 \pm 1^\circ$ of the magnetic field axis.

To provide a simple model for the data of Fig. 1, it was assumed that the extinction (absorption plus scattering) cross-sections σ_{\parallel} and σ_{\perp} (for light with ϵ parallel and perpendicular to the nanotube, respectively) transform as those of a particle much smaller than the wavelength of light, namely

$$\sigma = (l^2 + m^2)\sigma_{\perp} + n^2\sigma_{\parallel}, \quad (1)$$

where l and m are the direction cosines from ϵ to the short principal axes of the nanotube, and n is the direction cosine to its long axis. By averaging over the angular distribution of nanotubes, we obtain effective cross-sections for $\epsilon \parallel \mathbf{B}$ and $\epsilon \perp \mathbf{B}$ of

$$\bar{\sigma}_{\parallel} = \sigma_{+} + \sigma_{-} [u^{-2}v^{-1}(u-v) - 1], \quad (2)$$

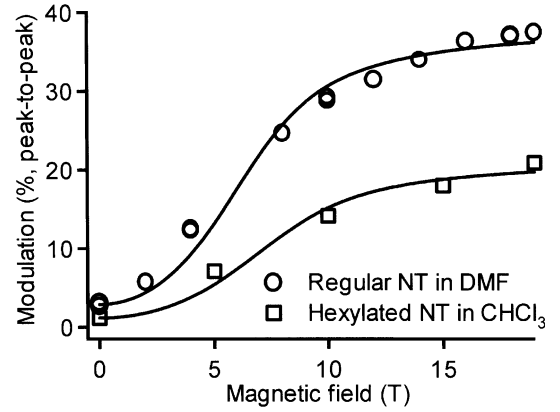


Fig. 2. Peak-to-peak modulation amplitude, as a fraction of average transmittance, vs. field for unmodified SWNTs (circles). The solid line is a two-parameter fit assuming a monodispersed ((10,10) tubes, 300 nm length) suspension of SWNTs. The modulation at zero field was subtracted before fitting. Based on the fit parameters, the average nanotube experienced an alignment energy of $(28 \pm 3)k_B T$ at 19 T. Nanotubes with hexyl groups covalently attached to their sidewalls (squares) required higher fields to achieve the same degree of measured alignment and produced lower modulations of intensity, owing to disruption of the π -bonding network.

and

$$\bar{\sigma}_{\perp} = \sigma_{+} - \sigma_{-} [(1/2)u^{-2}v^{-1}(u-v)], \quad (3)$$

where $\sigma_{\pm} = (\sigma_{\parallel} \pm \sigma_{\perp})/2$. Combining these with the transmittance T of a thickness t of a medium containing N scatterers per unit volume, $T = \exp(-Nt\sigma)$, and defining the peak-to-peak modulation M as $2Q/P$ where $T = P + Q \sin(R\theta + S)$, we obtain a modulation of

$$M = \tanh(A[(3/2)u^{-2}v^{-1}(u-v) - 1]) \quad (4)$$

in which the constant $A = Nt\sigma_{-}/2$. Parameters from the fit of Fig. 2 yield a cross-section anisotropy $\sigma_{\parallel} - \sigma_{\perp} = 10.9 \pm 1.5 \text{ nm}^2$.

Similar measurements were made with a chloroform suspension of nanotubes whose sidewalls had been covalently derivatized with hexyl groups [13]. Bonds to these side chains disrupt the network of conjugated π -bonds which determine the electronic structure of the nanotubes, and this disruption is likely to change their magnetic susceptibilities. The derivatized nanotubes required higher fields for alignment, but good alignment was still obtained (Fig. 2).

We produced the first macroscopic solid membranes of aligned tubes by filtering a nanotube/Triton-X suspension onto a porous membrane arranged parallel to the 25 T magnetic field vector. Two Millipore (Bedford, MA) Millex-GN syringe filters, each having a 25 mm diameter nylon membrane with 0.2 μm pores, were connected in parallel, primed with 0.05% Triton-X in ultrapure water, then suspended in a 27 T, 50 mm bore electromagnet. A sonicated suspension of 20–40 mg/l purified single-wall nanotubes in Triton-X suspension was flowed through the filters under a constant pressure of 20 psi. After the desired amount of suspension had passed through (measured by continuously weighing the filtrate), the flow was switched to a water/Triton-X solution with no nanotubes. The liquid circulating through the apparatus was then gradually changed to isopropyl alcohol (IPA) by means of a mixing chamber, initially full of water/Triton-X solution, of volume ~ 15 ml. IPA was allowed to flow for at least 15 min to remove the residual Triton-X. When the rinses with solvent and IPA were omitted, the nanotubes remained in a concentrated liquid suspension at the filter surface but did not consolidate. This suggests that removal of the surfactant is necessary for the nanotubes to coalesce into a firm filter cake.

3. Results and discussion

The black film that deposited onto the filter (Fig. 3) was more reflective than a typical filter cake (also sometimes called ‘buckypaper’) produced at zero field. More notably, it cleaved along a direction parallel to that of the ambient magnetic field axis during the filtration process, producing long ribbons with straight edges (Fig. 4), in contrast to buckypapers made at zero field, which tear with a ragged edge in every direction. This exhibition of natural cleavage planes implies highly anisotropic strength, maximal in the field direction. The freshly exposed surface of a ribbon consists of bands of tightly packed SWNTs; in comparison, normal papers appear as a tangle of separate, well-defined SWNT ropes [14]. Density measurements indicate that the aligned samples

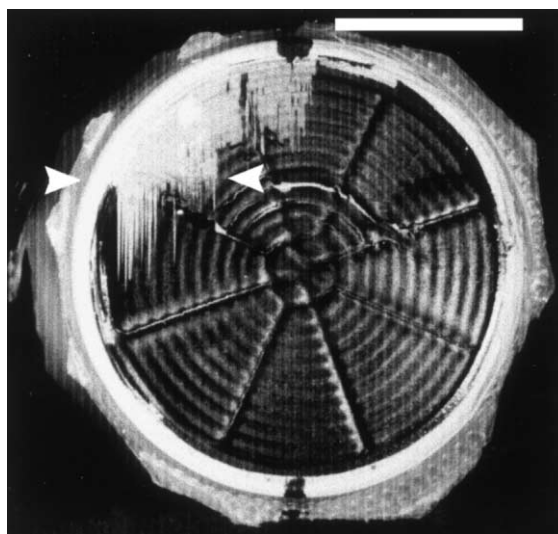


Fig. 3. In-plane-aligned assembly of SWNTs, formed by filtration in a 25 T magnetic field (field axis is marked by dots at perimeter of filter). At upper left, the membrane was removed from the filter surface using adhesive tape. Ribbons of aligned SWNTs peeled up from the surface past the location of the edge of the tape (arrowheads). Due to cleavage of the membrane, these ribbons have straight edges parallel to the field axis. This indicates that the membrane is strong along the magnetic field axis and weak transverse to it. The nanotube suspension consisted of 38.5 mg/l nanotubes in a 0.05% solution of Triton X-100 in water. Eight assemblies were produced with similar results. Scale bar, 1 cm.

are about 50% that of the close-packing limit that would obtain for (10, 10) tubes stacked parallel to one another in hexagonally closest packed array.

The aligned SWNT membranes were observed to have unusual optical properties. When the diffuse reflection of unpolarized light from an aligned membrane was viewed through a polarizer, its intensity was maximal when the polarization was along the magnetic field axis and minimal when the polarization was perpendicular to the field axis. This is consistent with the polarization dependence of scattering described above. Raman spectra (Fig. 5) showed a higher scattering intensity, by a factor of 7 ± 2 , when the polarization of the incident and detected light was parallel to the field axis rather than perpendicular. A piece of aligned nanotube assembly was removed from the filter membrane using adhesive tape. Another piece of adhesive tape was pressed on top of the

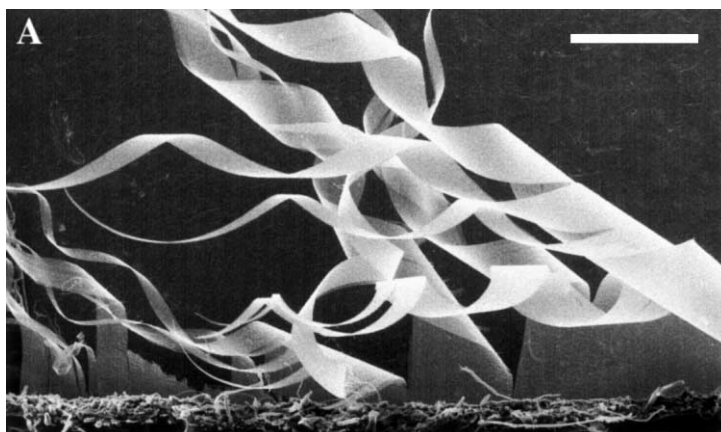


Fig. 4. Scanning electron micrograph of ribbons of aligned SWNTs peeled from the sample of Fig. 3. The tape is visible at the bottom of the image. Curling of the ribbons is due to nonuniform stresses during peeling, just as wrapping ribbon is curled by scraping with scissors (membranes that are released by dissolving the filter remain flat). Scale bar, 500 μm .

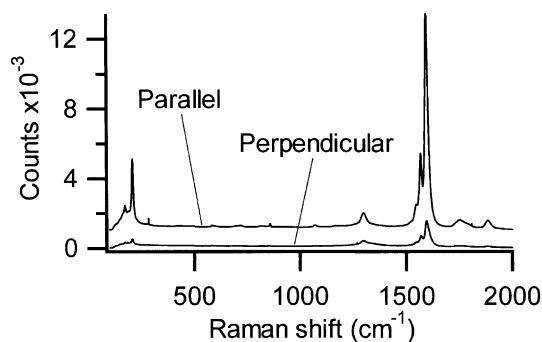


Fig. 5. Representative Raman scattering spectrum of a 2 μm spot on the cleaved surface of an aligned nanotube assembly, with the incident polarization parallel and perpendicular to the magnetic field axis. Observed at five locations, the scattering signal was (7 ± 2) times stronger with the polarization parallel to the field axis. The parallel trace has been shifted upwards by 1000 counts.

assembly smoothly and gently then pulled off to expose a fresh interior surface. The Raman spectrum was collected using a Renishaw (Schaumburg, IL) Micro-Raman System 1000 in Extended mode with a $20\times$ objective and a 780 nm diode laser for excitation. Total collection time was 90 s. The quoted intensity ratio is for the peak at $\sim 1580\text{ cm}^{-1}$. Unexpectedly, the spectra appear similar except for an overall scale factor. Theory predicts that some peaks should grow and others shrink as the polarization is rotated [15]. Such

changes in peak ratios may, however, be obscured by the distribution of chiralities present.

Aggressive sonication of purified SWNT samples in surfactants such as Triton-X or highly polar solvents like dimethyl formamide, does, however, produce a suspension of SWNTs containing mostly individuals and a few small bundles. One can easily deposit the tubes from such a suspension on a silicon wafer coated with a self-assembled monolayer that has an amine termination [16]. In addition to revealing that most tubes deposited from suspension are in the form of individuals and small bundles, this deposition technique also permits a direct measurement of the length distribution of the suspended SWNT using an atomic force microscope [16]. For the tubes used in the present experiment, the length distribution is centered at about 200 nm, and primarily contains tubes of lengths between 100 and 500 nm. (Such AFM studies now reveal that the length distributions from Triton-X suspensions of laser-oven nanotubes that have merely been sonicated to disperse and suspend the tubes are similar to length distributions reported previously [17] following sonication in a highly oxidizing environment. The realization that most nanotubes from Tubes@Rice have lengths between 100 and 500 nm has clear implications for measurements of rope properties such as strength, and electrical and thermal conductivities.)

Filtered nanotubes, which are the product of the current experiment, are usually observed in the form of ‘ropes’ of substantially larger diameter than the individual tubes and bundles observed by wafer deposition. It is of interest to understand how the aligned SWNTs bundle together into ropes during filtration even in the absence of a magnetic field, as this understanding may point to means of achieving denser arrays by aligning tubes in a magnetic field. Nanotubes have a terrific propensity to form ropes of 10–100 nanotubes when filtered or otherwise extracted from suspensions in which most tubes are individuals and small ropes. Surfactants (Triton-X appears to be the best we have examined) reduce the nanotubes’ surface free energy to produce the metastable state of individual tubes in suspension; sonication provides the energy required to exfoliate tubes.

Given frequent enough collisions, such as those occurring during filtering in the highly concentrated region 10–100 μm above the filter, two individual nanotubes can interpenetrate each other’s surfactant layers and stick together, enthalpically driven by the very large tube–tube van der Waals binding energy (~ 0.5 eV/nm length). Barriers to sliding an SWNT axially along a rope are small, permitting individual SWNTs to pack into a long rope with a uniform diameter, as observed. The volume just above the filter membrane, where the SWNT concentration, and thus their collision frequency, increase dramatically, is the region where rope formation occurs, producing the ropes typically observed from filtration. Roping up in this way is evidently quite facile; this process, together with the apparently short nascent lengths, should be kept in mind when looking at long, uniform diameter ropes. They do *not* consist in continuous tubes over a substantial fraction of the rope length.

Similar roping behavior should occur when magnetically aligned tubes enter this concentrated region immediately above the filter membrane. The degree of alignment achieved will depend on the nanotube concentration, and the competition between the magnetic field and shear fields set up by the filtering. One crucial difference between random and magnetically aligned roping needing further examination is the possibility that the concentration of aligned tubes may increase in this

volume above that required to form a nematic liquid crystal phase. This may have significant consequences for aligning and spinning aligned fibers from nanotube suspensions, or perhaps even from simple dispersions.

4. Conclusion

Production of aligned SWNT assemblies is also possible using superconducting or permanent magnets, rather than the inefficient resistive-coil magnets used in the investigations reported here. Since the alignment energy is proportional to the number of moles of carbon, a rope of nanotubes actually requires less magnetic field for alignment than an individual nanotube of the same length. Therefore, if we can control the filtration process to form ropes gently without misaligning or tangling them, a much lower field may suffice, making aligned nanotubes widely available. We have already produced excellent aligned membranes using a 7 T superconducting magnet. In addition to magnetic fields, it may be possible to obtain macroscopically aligned nanotube materials by applying shear or elongation fields, or by slow crystallization from solution.

Additional characterization of these aligned nanotube assemblies will determine their degree of crystallinity and their electronic, thermal, optical, mechanical, and magnetic properties. The present work is a step toward obtaining nanotube materials that fully exploit their remarkable properties. One overarching challenge that is partially enabled by aligned nanotubes is organized growth. By using the cut end of an aligned SWNT membrane as a seed crystal or catalyst template for further growth, it may be possible to produce a cable of continuous nanotubes – a macroscopic material whose nanoscale organization would give it the outstanding strength and other properties approaching those of individual nanotubes.

Acknowledgements

We gratefully thank Drs. J. Crow, B. Brandt, V. Salters, T. Zateslo, and the entire excellent staff of

the NHMFL for their assistance; and the Office of Naval Research (grant #N00014-99-1-0246), the National Aeronautics and Space Administration (award #NCC 9-77), and the Welch Foundation for financial support. A portion of this work was performed at the National High Magnetic Field Laboratory, which is supported by NSF Cooperative Agreement No. DMR-9527035 and by the State of Florida.

References

- [1] J.P. Lu, *Phys. Rev. Lett.* 74 (1995) 1123.
- [2] I. Yamashita, H. Suzuki, K. Namba, *J. Mol. Biol.* 278 (1998) 609.
- [3] A. Fujiwara, H. Ootoshi, H. Suematsu, M. Yumura, K. Uchida, in: S. Fujiwara, et al. (Eds.), *Super Carbon*, MY, Tokyo, 1998, p. 73.
- [4] L. Wang, P.S. Davids, A. Saxena, A.R. Bishop, *J. Phys. Chem. Solids* 54 (1993) 1493.
- [5] H. Ajiki, T. Ando, *J. Phys. Soc. Jpn.* 62 (1993) 2470.
- [6] R.C. Haddon, A. Pasquarello, *Phys. Rev. B* 50 (1994) 16459.
- [7] S.-I. Zhu, Y.-C. Zhou, *Solid State Commun.* 95 (1995) 765.
- [8] M.F. Lin, K.W.K. Shung, *Phys. Rev. B* 52 (1995) 8423.
- [9] M. Abramowitz, I.A. Stegun, *Handbook of Mathematical Functions*, Dover, New York, 1965.
- [10] A. Thess, R. Lee, P. Nikolaev, H.J. Dai, P. Petit, J. Robert, C.H. Xu, Y.H. Lee, S.G. Kim, A.G. Rinzler, D.T. Colbert, G.E. Scuseria, D. Tománek, J.E. Fischer, R.E. Smalley, *Science* 273 (1996) 483.
- [11] A.G. Rinzler, J. Liu, H. Dai, P. Nikolaev, C.B. Huffman, F.J. Rodriguez-Macias, P.J. Boul, A.H. Lu, D.T. Colbert, R.S. Lee, J.E. Fischer, A.M. Rao, P.C. Eklund, R.E. Smalley, *Appl. Phys. A (Mater. Sci. Process.)* 67 (1998) 29.
- [12] See H.C. van de Hulst, *Light scattering by small particles*, Dover, New York, 1981 (for a treatment of the electromagnetic properties of thin metallic rods).
- [13] P.J. Boul, et al., *Chem. Phys. Lett.* 310 (1999) 367.
- [14] A.G. Rinzler, J. Liu, H. Dai, P. Nikolaev, C.B. Huffman, F.J. Rodriguez-Macias, P.J. Boul, A.H. Lu, D.T. Colbert, R.S. Lee, J.E. Fischer, A.M. Rao, P.C. Eklund, R.E. Smalley, *Appl. Phys. A (Mater. Sci. Process.)* 67 (1998) 29.
- [15] R. Saito, T. Takeya, T. Kimura, G. Dresselhaus, M.S. Dresselhaus, *Phys. Rev. B* 57 (1998) 4145.
- [16] J. Liu, M.J. Casavant, M. Cox, D.A. Walters, P. Boul, W. Lu, A.J. Rimberg, K.A. Smith, D.T. Colbert, R.E. Smalley, *Chem. Phys. Lett.* 303 (1999) 125.
- [17] J. Liu, A. Rinzler, H. Dai, J. Hafner, R. Bradley, A. Lu, K. Shelimov, C. Huffman, F. Rodriguez-Macias, P. Boul, T. Iverson, D.T. Colbert, R.E. Smalley, *Science* 280 (1998) 1253.